View metadata, citation and similar papers at core.ac.uk

brought to you by CORE

provided by Repositorio da Producao Cientifica e Intelectual da Unicamp

Electron and positron scattering from 1 , 1 - C 2 H 2 F 2

C. Makochekanwa, H. Kato, M. Hoshino, M. H. F. Bettega, M. A. P. Lima, O. Sueoka, and H. Tanaka

Citation: The Journal of Chemical Physics **126**, 164309 (2007); doi: 10.1063/1.2723738

View online: http://dx.doi.org/10.1063/1.2723738

View Table of Contents: http://scitation.aip.org/content/aip/journal/jcp/126/16?ver=pdfcov

Published by the AIP Publishing

Articles you may be interested in

Total, elastic, and inelastic cross sections for positron and electron collisions with tetrahydrofuran
J. Chem. Phys. **138**, 074301 (2013); 10.1063/1.4789584

A comparative study of electron and positron scattering from chlorobenzene (C 6 H 5 Cl) and chloropentafluorobenzene (C 6 F 5 Cl) molecules
J. Chem. Phys. **119**, 12257 (2003); 10.1063/1.1626115

A comparative study of electron and positron scattering from molecules. IV. CH 3 Cl , CH 3 Br , and CH 3 I molecules
J. Chem. Phys. **115**, 7442 (2001); 10.1063/1.1402996

Vibrational excitation of carbon oxysulfide molecules by positron and electron impacts
J. Chem. Phys. **112**, 7057 (2000); 10.1063/1.481302

Remarks on total and elastic cross sections for electron and positron scattering from CO 2
J. Chem. Phys. **107**, 6616 (1997); 10.1063/1.474903

This article is copyrighted as indicated in the article. Reuse of AIP content is subject to the terms at: http://scitation.aip.org/termsconditions. Downloaded to IP: 143.106.108.187 On: Thu, 18 Jun 2015 19:20:36

Electron and positron scattering from 1,1-$C_2H_2F_2$

C. Makochekanwa[a)]
Physics Department, Sophia University, Chiyoda-ku, Tokyo 102-855, Japan and Faculty of Engineering, Yamaguchi University, Yamaguchi 755-8611, Japan

H. Kato and M. Hoshino
Physics Department, Sophia University, Chiyoda-ku, Tokyo 102-855, Japan

M. H. F. Bettega
Departamento de Física, Universidade Federal do Paraná, Caixa Postal 19044, 81531-990 Curitiba, Paraná, Brazil

M. A. P. Lima
Instituto de Física "Gleb Wataghin," Universidade Estadual de Campinas, 13083-970 Campinas, São Paulo, Brazil

O. Sueoka
Faculty of Engineering, Yamaguchi University, Yamaguchi 755-8611, Japan

H. Tanaka
Physics Department, Sophia University, Chiyoda-ku, Tokyo 102-855, Japan

(Received 20 February 2007; accepted 15 March 2007; published online 25 April 2007)

1,1-difluoroethylene (1,1-$C_2H_2F_2$) molecules have been studied for the first time experimentally and theoretically by electron and positron impact. 0.4–1000 eV electron and 0.2–1000 eV positron impact total cross sections (TCSs) were measured using a retarding potential time-of-flight apparatus. In order to probe the resonances observed in the electron TCSs, a crossed-beam method was used to investigate vibrational excitation cross sections over the energy range of 1.3–49 eV and scattering angles 90° and 120° for the two loss energies 0.115 and 0.381 eV corresponding to the dominant C–H (ν_2 and ν_9) stretching and the combined C–F (ν_3) stretching and CH_2 (ν_{11}) rocking vibrations, respectively. Electron impact elastic integral cross sections are also reported for calculations carried out using the Schwinger multichannel method with pseudopotentials for the energy range from 0.5 to 50 eV in the static-exchange approximation and from 0.5 to 20 eV in the static-exchange plus polarization approximation. Resonance peaks observed centered at about 2.3, 6.5, and 16 eV in the TCSs have been shown to be mainly due to the vibrational and elastic channels, and assigned to the B_2, B_1, and A_1 symmetries, respectively. The π^* resonance peak at 1.8 eV in C_2H_4 is observed shifted to 2.3 eV in 1,1-$C_2H_2F_2$ and to 2.5 eV in C_2F_4; a phenomenon attributed to the decreasing C=C bond length from C_2H_4 to C_2F_4. For positron impact a conspicuous peak is observed below the positronium formation threshold at about 1 eV, and other less pronounced ones centered at about 5 and 20 eV. © *2007 American Institute of Physics*. [DOI: 10.1063/1.2723738]

I. INTRODUCTION

Perfluorocarbon (C_mF_n) molecules have long been regarded as important and efficient gases for plasma etching. However, because of the impact of their long lifetimes in the stratosphere on climate, the need for replacement with safer gases is called for. $C_2H_2F_2$, C_2OF_2, and CF_3I are among the nonperfluorocarbons whose CF_n radicals can be of great use for applications, and have thus been proposed as replacement gases.[1,2] In line with this we have carried out the first steps towards creating a cross section data set for this possibly industrially relevant species. In addition, from a physical and chemical point of view, the 1,1-difluoroethylene (1,1-$C_2H_2F_2$) molecules we study here are of interest since they have the peculiar intramolecular forces, molecular structure, and scattering dynamics of F-containing molecules supposedly lying midway between the pure hydrocarbon C_2H_4 and the pure perfluorocarbon C_2F_4.

Though C_2H_4, and C_2F_4 have received considerable attention by both experimentalists (e.g., see Refs. 3 and 4) and theorists (e.g., see Refs. 5 and 6), to our knowledge there are no relative or absolute cross section data for either electron or positron interactions with 1,1-$C_2H_2F_2$ available in literature, except for electron impact excitation transition energies and term value studies carried out systematically for the whole series of fluoroethylenes from C_2H_3F up to C_2F_4.[7] The dominating theme in most of these previous studies on C_2H_4 and C_2F_4 has been the observations of the π^* shape resonance that has been systematically observed to be a feature arising due to the C=C double bond in the molecular struc-

[a)]Author to whom correspondence should be addressed. Present address: Atomic and Molecular Physics Laboratories, RSPhysSE, The Australian National University, Canberra ACT 0200, Australia. Electronic mail: cxm107@rsphysse.anu.edu.au

 © 2007 American Institute of Physics

This article is copyrighted as indicated in the article. Reuse of AIP content is subject to the terms at: http://scitation.aip.org/termsconditions. Downloaded to IP: 143.106.108.187 On: Thu, 18 Jun 2015 19:20:36

tures of these molecules. It is worthwhile, however, to note that there exist some Raman spectra[8–10] works that studied the vibrational frequencies, and microwave spectra[11] studies that established the bond lengths, bond angles, and dipole moments, in literature for 1,1-$C_2H_2F_2$ molecules. Far-ultraviolet spectra were also studied for these molecules, along with the whole series of other fluoroethylenes: C_2H_4, C_2H_3F, *cis*-1,2-$C_2H_2F_2$, *trans*-1,2-$C_2H_2F_2$, 1,1-$C_2H_2F_2$, C_2HF_3, and C_2F_4, wherein the authors systematically studied the $\pi \rightarrow \pi^*$ transitions and discovered that this series of molecules exhibited fine vibrational structure clearly dominated by the C=C stretching and twisting vibrations. Also related to these studies are the experiments by Allan *et al.*[12] who carried out investigations of the dipole moment effect on the threshold peaks of the vibrational excitation of *cis*- and *trans*-1,2-$C_2H_2F_2$ by electron impact.

The comparative study between electron and positron cross sections we carry out in this study aids in even better understanding of the electron cross sections themselves. In addition, besides the established applications of positron scattering to areas such as positron emission tomography[13] and characterization of materials,[14] recent predictions of positron bound states with neutral atoms have also increased interest in the areas of positron and positronium chemistry,[15] so that any fingerprints of this in polyatomic molecules will be an invaluable advance to physics and chemistry.

In the present work we report on measurements of total and vibrational excitation cross sections for electron collisions with 1,1-$C_2H_2F_2$, as well as on computational studies of the corresponding integral elastic cross sections. We also report measurements of total cross sections (TCSs) for positron collisions with this gas. This collision data set should be useful in understanding the basic physics and possible applications of these molecules.

II. EXPERIMENTAL PROCEDURE

A. Total cross sections

The electron and positron scattering TCSs were measured over the energy range of 0.2–1000 eV using a retarding potential time-of-flight (RP-TOF) apparatus that we have described in earlier publications,[16] and thus it is only summarized here. A ^{22}Na radioisotope with an activity of 80–100 μCi is used for both the positron and electron sources. In order to obtain the slow positron beam a moderator consisting of a set of seven-overlapping tungsten meshes baked at 2100 °C is used. The energy resolution of the RP-TOF experimental apparatus is ~0.3 eV at impact energies below 5 eV, and varies with impact energy as shown in Ref. 17. The TCS values, Q_t, were derived from the Beer-Lambert equation

$$Q_t = -\frac{1}{n\ell}\ln\left(\frac{I_v}{I_g}\right) \quad (1)$$

where I_g and I_v refer to the projectile beam intensities transmitted through the collision cell with and without the target gas of number density n, respectively. ℓ refers to the effective length of the collision cell and was established by normalizing our measured positron-N_2 TCSs to those of the positron-N_2 data of Hoffman *et al.*[18] Separate experiments were carried out at electron energies of 10 eV (*i.e.*, in the resonance region) and at 200 eV to check the pressure independence of the 1,1-$C_2H_2F_2$ TCS data presented here. The results of these test experiments confirmed this independence. Target gas pressures used in these measurements were between 2 and 6 mTorr. The energy scale was calibrated using the positron-N_2 TOF spectra measured at 20 energies in the randomly chosen region of 8–150 eV.[19]

The present apparatus setup has specifically been designed to have a collision cell with 3 mm radius entrance and exit apertures for the weak positron beam intensities, i.e., for positron scattering experiments. Thus the ceratron detector can detect some projectiles scattered through small angles, when it should only detect the unscattered signal, i.e., the so-called forward scattering effect. It therefore becomes necessary to account for any such effects for correct TCS values. The procedure for this, which takes into account the molecular differential cross sections (DCSs) and collision cell geometry, has been described in detail in our previous publications.[16,17,19,20] For these molecules, however, neither electron nor positron DCSs were available and so this correction could not be done. It is worth pointing out though that from our experience the forward scattering correction, if at all done, only increases the TCS magnitudes by a few percent and does not affect the type of structures we observe, and thus our results and the discussions presented here are credible and useful for applications.

The errors shown in the data in Table I are the total uncertainties, made up of statistical, pressure fluctuations, and collision cell effective length determination, amounted to a maximum of 7% for electron impact and 12% for positron impact.

B. Vibrational excitation cross sections

The crossed-beam apparatus used in the present differential cross section functions for vibrational excitation measurements is the same as that used in our previous studies.[21] Briefly summarized, the apparatus consists of a monochromator and an analyzer both enclosed in differentially pumped boxes to reduce the effect of the background gases and stray electron backgrounds. The molecular beam was produced by continually effusing the 1,1-$C_2H_2F_2$ gas through a nozzle with an internal diameter of 0.3 mm and length of 5 mm. The spectrometer and nozzle were heated to a temperature of about 70° to avoid sticking of the gas sample. Helium was used as the reference gas in the relative flow technique.[22] The electron energy scale was calibrated with respect to the 19.367 eV resonance in He. Gas sample pressures for these measurements were about 4 Torr. The overall energy resolution was about 35–40 meV (full width at half maximum) while the angular resolution was ±1.5°. Overall experimental errors in the DCS functions were estimated to be about 20%.

III. THEORETICAL PROCEDURE

To compute the elastic integral cross sections (ECSs) we employed the Schwinger multichannel[23] (SMC) method with pseudopotentials.[24] Details about this method can be found

This article is copyrighted as indicated in the article. Reuse of AIP content is subject to the terms at: http://scitation.aip.org/termsconditions. Downloaded to IP: 143.106.108.187 On: Thu, 18 Jun 2015 19:20:36

TABLE I. 1,1-$C_2H_2F_2$ electron and positron TCSs (10^{-16} cm^2). The errors are as explained in the text.

Energy (eV)	Electron	Positron	Energy (eV)	Electron	Positron
0.2		7.5±0.9	11	23.1±1.3	13.1±0.9
0.4	18.3±1.3	9.1±0.9	12	23.1±1.3	13.0±1.0
0.6	17.8±1.1	11.3±1.0	13	23.3±1.3	14.0±1.0
0.8	17.4±1.1	12.1±1.0	14	23.6±1.3	13.9±1.1
1.0	18.1±1.1	12.7±1.0	15	23.8±1.3	13.7±1.1
1.2	18.4±1.1		16	23.7±1.3	14.2±1.2
1.3		12.0±0.9	17	23.8±1.3	14.4±1.1
1.4	19.4±1.1		18	23.6±1.3	14.5±1.1
1.6	20.4±1.2	12.3±0.9	19	22.9±1.3	14.9±1.1
1.8	22.2±1.3		20	22.5±1.3	14.8±1.2
1.9		11.9±0.9	22	21.5±1.2	14.6±1.0
2.0	23.5±1.4		25	20.8±1.2	14.4±1.1
2.2	25.8±1.5	11.6±0.9	30	19.8±1.1	14.5±1.0
2.5	25.6±1.5	11.6±0.9	35	19.6±1.1	
2.8	24.9±1.5	12.0±0.9	40	21.0±1.1	14.2±1.0
3.1	23.3±1.3	12.8±1.0	50	20.0±1.1	14.2±1.0
3.4	22.1±1.3	12.0±0.9	60	18.2±1.0	13.1±0.9
3.7	21.9±1.2	13.1±1.0	70	17.5±1.0	12.9±1.0
4.0	21.9±1.3	13.1±0.9	80	16.6±0.9	12.2±1.3
4.5	23.6±1.4	13.1±0.9	90	15.7±0.9	11.8±0.8
5.0	24.5±1.4	13.2±0.9	100	14.8±0.8	12.1±1.0
5.5	25.4±1.4	13.1±0.9	120	13.9±0.8	11.2±0.9
6.0	25.5±1.4	12.8±1.0	150	12.5±0.7	10.7±0.8
6.5	25.7±1.4	13.9±1.0	200	10.6±0.6	10.3±0.8
7.0	25.1±1.4	13.3±1.0	250	9.8±0.5	8.2±0.7
7.5	24.9±1.4	12.9±1.0	300	8.3±0.5	7.9±0.6
8.0	24.5±1.4	13.7±1.0	400	7.0±0.4	6.4±0.6
8.5	24.1±1.4	13.2±1.0	500	6.2±0.3	6.1±0.5
9.0	23.9±1.4	12.7±1.0	600	5.2±0.3	5.4±0.5
9.5	23.4±1.3	13.2±1.0	800	4.6±0.3	4.4±0.4
10	23.1±1.3	13.2±0.9	1000	3.8±0.2	3.7±0.4

in these previous publications and thus we will only describe here those points directly relevant to the calculations for the 1,1-$C_2H_2F_2$ molecules presented in this paper.

Our calculations were carried out at the ground state equilibrium geometry in the static-exchange and in the static-exchange plus polarization approximations. The basis set used in the bound state and in the scattering calculations for C and F atoms can be found in Ref. 25 and, in Ref. 26 for H atoms. Although this molecule has a permanent dipole moment (1.648 D in the present calculation), we have not used a Born closure scheme to account for the higher angular momentum components of the scattering amplitude. For the present energy range, previous calculations have shown that the truncated SMC scattering amplitude gives similar results (resonance positions and even cross section magnitudes) than those obtained by properly accounting for the long-range part of the dipole moment.[27]

We included polarization effects in order to improve the position of the shape resonances in the A_1, B_1, and B_2 symmetries, while A_2 was computed in the static-exchange approximation only, since its cross section is small. For the A_1 and B_1 symmetries we included polarization effects through single excitations of the target from the occupied (valence) orbitals to a set of polarized orbitals, generated as described in Ref. 28. We included 6091 configuration state functions (CSFs) for A_1 and 4852 CSFs for B_1. Since there is a sharp shape resonance in the B_2 symmetry, we included polarization in this symmetry using the procedure described in Ref. 29. We included all single excitations that preserved the spatial symmetry of the molecular ground state (A_1 in this case), from the occupied orbitals to the unoccupied (virtual) orbitals, and used a modified virtual orbital[30] as the scattering orbital. We included all singlet and triplet coupled CSFs, obtaining 1413 CSFs for this symmetry. For A_2 we included only the 13 CSFs in the static-exchange approximation.

IV. RESULTS AND DISCUSSION

The values for both electron and positron TCSs are shown in Table I.

A. Electron impact

1. 1,1-$C_2H_2F_2$

Figure 1 shows the current electron impact TCS results measured over the energy range of 0.4–1000 eV. These results are characterized by the gradually rising trend below 0.8 eV, peaks centered at about 2.3, 6.5, 16, and 40 eV, before the rather rapidly decreasing trend above this energy towards 1000 eV, i.e., from about 26×10^{-16} cm^2 (at 2.3 and 6.5 eV) down to about 4×10^{-16} cm^2 at 1000 eV. The rising

This article is copyrighted as indicated in the article. Reuse of AIP content is subject to the terms at: http://scitation.aip.org/termsconditions. Downloaded to IP: 143.106.108.187 On: Thu, 18 Jun 2015 19:20:36

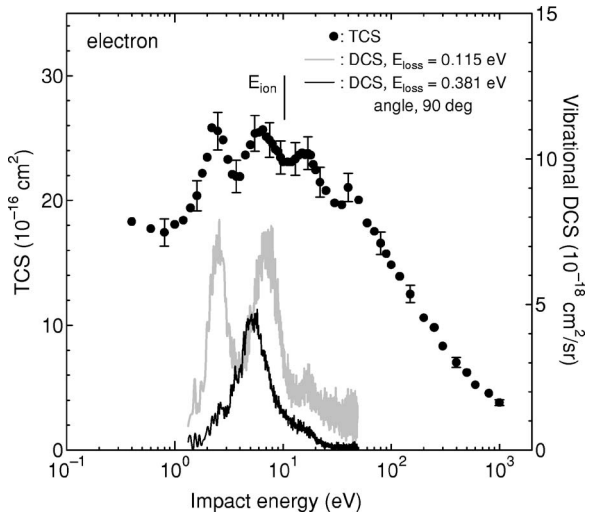

FIG. 1. Present 1,1-$C_2H_2F_2$ electron scattering TCSs and vibrational excitation DCSs for the two dominant modes C–H stretching (E_{loss}=0.381 eV) and the combined C–F stretching and CH_2 rocking (E_{loss}=0.115 eV) vibrations. Note that the vertical scale for the vibrational excitation DCSs is on the right hand side. The vertical bar labeled E_{ion} shows the position corresponding to the threshold for ionization.

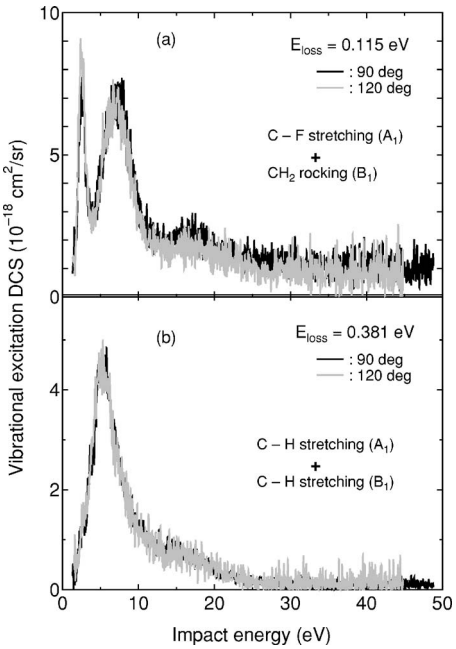

FIG. 3. Electron impact 1,1-$C_2H_2F_2$ vibrational excitation DCSs at the energy losses of 0.115 and 0.381 eV.

trend below 0.8 eV can be attributed to the enhanced forward scattering due to the presence of the relatively large dipole moment (1.368 D for the experimental literature value[31] and 1.648 D for the present computed value) and polarizability (5.01×10^{-30} m^3 for the experimental literature value[31] and 4.00×10^{-30} m^3 for the present computed value). The decreasing trend above 40 eV is due to the decreasing time the electron has for interaction with the molecule as its velocity increases. However, the origin and nature of the above mentioned peaks cannot be put forward with any certainty unless carefully probed. As tools for this, we carried out a combination of vibrational excitation measurements, i.e., study the inelastic channel often associated with resonance features of this nature, and the theoretical study of the elastic scattering channel.

Figure 2 shows the electron energy loss spectra for the

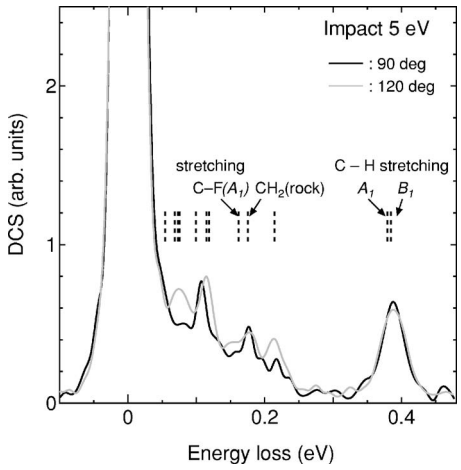

FIG. 2. Energy loss spectra for electron scattering from 1,1-$C_2H_2F_2$ molecules at the selected impact energy and scattering angles. The dashed vertical bars show the loss energy positions of the 12 fundamental vibrational modes.

impact energy of 5 eV and scattering angles of 90° and 120°. It is worth pointing out here that other measurements were also carried out at this energy for the scattering angles of 30° and 60°, though not shown here since they are similar to the ones shown. Similar measurements were also carried out at impact energies of 17, 7.5, and 2.5 eV and scattering angles of 30°, 60°, 90°, and 120°. Again the results are not shown since they are similar to the spectra presented in Figs. 2 and 3. Due to this similarity, we decided to focus the measurements at only these two angles. Like C_2H_4 and C_2F_4, 1,1-$C_2H_2F_2$ molecules have 12 fundamental vibrational modes,[9] and these are indicated by the dashed vertical bars in Fig. 2. The results we show in Fig. 3, and partly in Fig. 1, are for the vibrational excitation at the energy losses of 0.115 and 0.381 eV, chosen simply because these are some of the dominant modes and also because there is less mode congestion at these points, i.e., given the limitation due to our energy resolution of about 40 eV. The energy loss setting of 0.115 eV for our apparatus inevitably includes both the C–F (A_1) (ν_3) stretching (located at loss energy of 0.1149 eV) and the CH_2 (B_1) (ν_{11}) rocking (located at loss energy of 0.1184 eV) modes. Hence the following discussions of the 0.115 eV loss energy spectra ought to be interpreted as referring to a mixture of these two vibrational modes. Similarly, the setting of our apparatus for measurements at the energy loss of 0.381 eV inevitably means both symmetries of the C–H stretching mode are included, i.e., C–H (A_1) (ν_2) located at the loss energy of 0.3794 eV, and C–H (B_1) (ν_9) at 0.3847 eV, and thus the following discussions of the 0.381 eV spectra should be taken to mean the combination of the two. As shown in both Figs. 3(a) and 3(b), spectra taken for each loss energy at the two angles of 90° and 120° show nearly identical energy dependence features, and thus for the comparison of these vibrational cross sections with the TCSs in Fig. 1 we only use the results for one of these angles.

This article is copyrighted as indicated in the article. Reuse of AIP content is subject to the terms at: http://scitation.aip.org/termsconditions. Downloaded to IP: 143.106.108.187 On: Thu, 18 Jun 2015 19:20:36

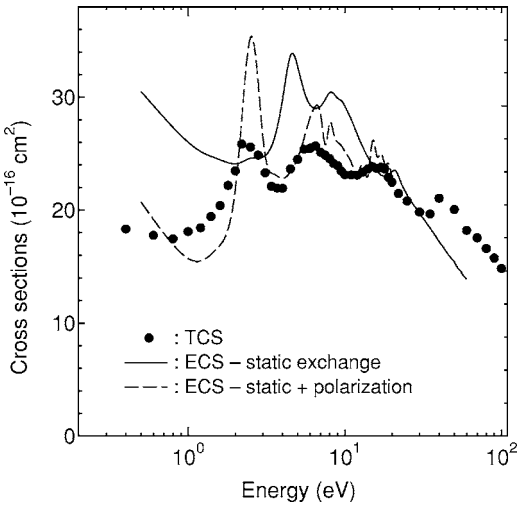

FIG. 4. Present electron impact experimental TCSs and the two theoretical SMC ECS results.

Note, however, that the vertical scale magnitudes of the TCSs and vibrational excitation DCSs (right hand side scale) are different in Fig. 1.

Allowing for the experimental uncertainties resulting in the rather noisy vibrational excitation cross section curves, there is clear agreement in the energy dependence between these spectra and the TCSs which we summarize as follows. (i) The 0.115 eV loss energy vibrational excitation cross sections show peaks centered at about 2.3, 6.5, 16, and the rather washed out one at around 40 eV, i.e., in complete agreement with the TCS peaks. (ii) The 0.381 eV loss energy cross sections are characterized by one peak centered at about 5.5 eV. It seems that the broad peak in the TCSs spanning the energy region from 4 to 10 eV is, in fact, a resonance feature composed of contributions from a mixture of these vibrational excitations. Because of the poor energy resolution of our TCS apparatus, about 0.5 eV in this region, we cannot resolve these individual peaks in the TCSs. Therefore, though here we do not present integral vibrational cross sections it is clear that the vibrational excitation channel is significantly contributing to the resonance features observed in the TCSs. It is important to point out though that we think the peak at about 40 eV observed in the TCSs should surely have stronger contributions from other scattering channels than the vibrational excitation, most likely ionization, owing to its rather weak contribution observed in the results we present in Figs. 1 and 3.

In Figs. 4 and 5 we present the results of the SMC calculations for the ECSs and the symmetry-resolved cross sections both at the static-exchange and static-exchange plus polarization scattering levels. We included polarization effects up to 20 eV, and for energies above that our results were computed only at the static-exchange approximation (except for A_2, as discussed above), since both approximations give practically equal results. In comparison with the experimental TCSs (Fig. 4) it is clear that inclusion of the polarization effects brings the calculated cross section in better agreement with the TCSs, which is shown by the better agreement in the resonance positions, i.e., a general shift to lower energies compared with the results obtained in the static-exchange approximation. Thus, despite the differences in magnitude between the TCSs and the static-exchange plus polarization ECSs, amounting to a maximum of 38% at 2.3 eV, these theoretical results support the existence of the shape resonances seen in the measured TCSs and vibrational excitation cross sections. Since our calculations were carried out in the fixed nuclei approximation, the magnitude of the cross section around the resonance is expected to be higher than the experimental value. Inclusion of nuclear motion lowers the magnitude of the resonance and broadens its width. Furthermore, a closer examination of the symmetry decomposition of the integral cross section (see Fig. 5) clearly shows that the cross sections for the B_2, B_1, and A_1 symmetries have peaks centered at about 2.4, 6.5, and 16 eV, respectively. That is, these symmetries are responsible for the resonances observed at the corresponding energy positions in the TCSs and vibrational excitation cross sections. Therefore,

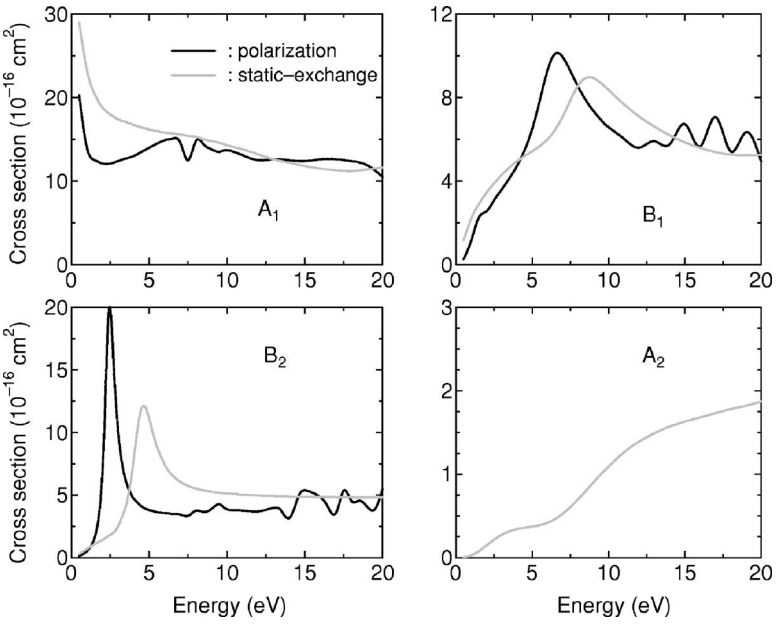

FIG. 5. The present SMC ECSs and the symmetry-resolved cross sections for both the static-exchange and static-exchange plus polarization approximation levels.

This article is copyrighted as indicated in the article. Reuse of AIP content is subject to the terms at: http://scitation.aip.org/termsconditions. Downloaded to IP: 143.106.108.187 On: Thu, 18 Jun 2015 19:20:36

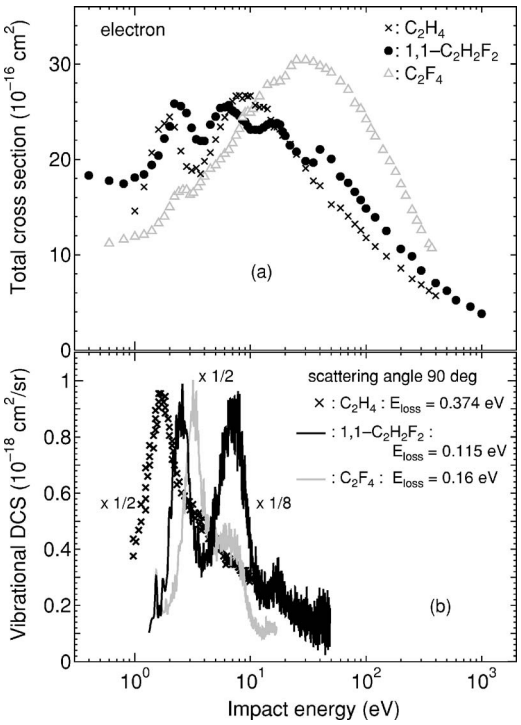

FIG. 6. TCSs and vibrational excitation DCSs for C_2H_4, 1,1-$C_2H_2F_2$, and C_2F_4 molecules.

the current theoretical results indeed correctly locate the resonance peaks and have identified the corresponding symmetries. We also noticed a minimum in the TCSs around 1 eV and in the ECSs around 1.5 eV. This minimum appears in the cross section of the A_1 symmetry, as shown in Fig. 5. We carried out the eigenphase sum analysis and found that this minimum is not a Ramsauer-Townsend minimum.

2. 1,1-$C_2H_2F_2$ compared with C_2H_4 and C_2F_4

Figures 6(a) and 6(b) show the current 1,1-$C_2H_2F_2$ TCSs and vibrational excitation cross sections compared with those for C_2H_4 and C_2F_4 molecules, i.e., a comparison that aids in investigating the effects of the two H atom substitutions in 1,1-$C_2H_2F_2$ and four H atoms in C_2F_4 compared to the "parent" C_2H_4 molecule. The C_2H_4 TCS and ECS results presented in this figure are from the experimental works of Refs. 32 and 3 respectively, while those for C_2F_4 are from Refs. 4 and 33, respectively. Here we are interested in the lowest energy resonance which is associated with the phenomenon observed to be characteristic of all C=C double bond containing hydrocarbons, and explained as due to the temporary trapping of the incoming electron into valance orbitals with the C=C antibonding character, i.e., the lowest unoccupied molecular orbital, which is a shape resonance (see, for example, Refs. 3 and 34). We infer that the 2.3 eV resonance observed in both 1,1-$C_2H_2F_2$ TCSs and vibrational excitation functions is due to this C=C double bond and that it too should be a shape resonance. It is interesting to note from this figure that though the 1,1-$C_2H_2F_2$ TCSs resemble more C_2H_4 TCSs than C_2F_4 TCSs, the vibrational excitation data show 1,1-$C_2H_2F_2$ better resembling C_2F_4 than C_2H_4.

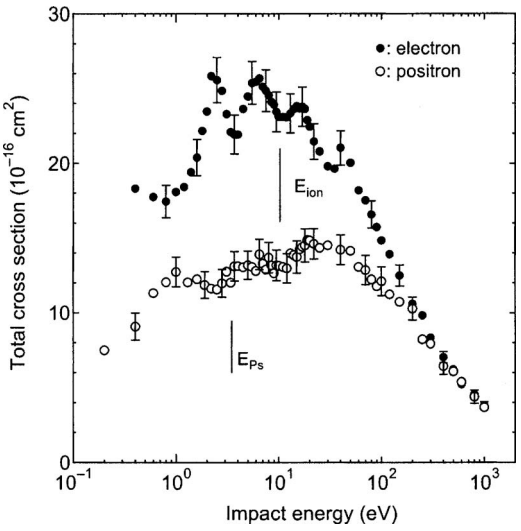

FIG. 7. Electron and positron TCSs for 1,1-$C_2H_2F_2$ molecules. The vertical bars show the positions corresponding to the threshold for positronium formation (E_{Ps}) and ionization (E_{ion}).

One more interesting phenomenon to be noted here is that, in both the TCSs [Fig. 6(a)] and vibrational excitation cross sections [Fig. 6(b)], the position of the shape resonance shifts as we move from C_2H_4, which is located at 1.8 eV, to 2.3 eV in 1,1-$C_2H_2F_2$ and 2.8 eV in C_2F_4. We also observed a similar phenomenon in a previous systematic study of the vibrational excitation cross sections for the CO based molecules CO, H_2CO, and F_2CO.[35] In that study this phenomenon was analyzed based on a model built upon the C=O bond lengths, i.e., which decreased in the order CO $<F_2CO<H_2CO$, when the peak energy positions were in the reverse order $CO>F_2CO>H_2CO$. Similar phenomena were also observed in electron impact studies on the fluoroethylenes, C_2H_4 to C_2F_4; whereby, (i) electron diffraction studies showed vibrational force constants correlating with the C=C bond lengths,[36] and (ii) ionization potential and electron affinities were observed to increase with increase in the C=C bond lengths, i.e., the C=C bond length shortening with increasing fluorination.[37] Since we observe a similar pattern to the above in the current series of molecules whereby the C=C bond length is 1.337 Å in C_2H_4, 1.316 Å in 1,1-$C_2H_2F_2$, and 1.311 Å in C_2F_4, i.e., in decreasing order as $C_2H_4>1,1\text{-}C_2H_2F_2>C_2F_4$, which is opposite to that of the peak energy positions, i.e., C_2H_4 (at 1.8 eV) $<1,1\text{-}C_2H_2F_2$ (at 2.3 eV) $<C_2F_4$ (at 2.8 eV), we therefore have drawn similar conclusions here, that is that the shorter the molecular bond length (internuclear distance) becomes, the deeper the potential barrier that the electron has to tunnel through, and thus the corresponding shape resonance energy is expected to become higher.

3. Positron TCSs: A comparative study with electron TCSs

In Fig. 7 we present the current 1,1-$C_2H_2F_2$ positron impact TCSs, in comparison with the just discussed electron TCSs. Whereas it was possible to present detailed discussions of the electron TCS features because of the availability of the experimental vibrational excitation and theoretical

This article is copyrighted as indicated in the article. Reuse of AIP content is subject to the terms at: http://scitation.aip.org/termsconditions. Downloaded to IP: 143.106.108.187 On: Thu, 18 Jun 2015 19:20:36

elastic integral cross sections, it is not possible to do the same here because of the lack of any partial cross sections for positron impact. The reason for this unavailability is in the difficulties involved in producing a stable and suitable positron beam to carry out such partial cross section measurements. Thus conclusive discussions still await joint experimental and theoretical partial cross sections, so that the following discussions are rather speculative but soundly based on currently established scattering physics.

The observed features are summarized as follows. (i) The positron TCSs decrease gradually below 1 eV, i.e., in contrast to the rising trend in the electron TCS counterpart at this energy range. The TCSs for both should rise at these low energies because of the large dipole moment and relatively large molecular polarizability and, if this long-range dipole interaction dominates, the two sets of TCS should behave similarly at these low energies. However, that we only observe this for electron impact and not positron impact clearly suggests the existence of a short-range interaction that is different for electron and positron, resulting in the different behaviors between the two TCSs. This raises an interesting and important question: At what energy will the positron TCSs increase at low energies and why is this energy different from that for electron TCSs? The answer to this should provide us with more basic knowledge of the interaction between 1,1-$C_2H_2F_2$ and these two projectiles. (ii) A conspicuous peak is observed centered at about 1 eV. This is interesting because it lies below the threshold for positronium formation, E_{Ps}, which is at 3.49 eV.[28] Although the exact origin and nature of this peak remain unknown, it may as well be due to contributions from rovibrational excitation, or positron attachment. In a previous systematic study of positron TCSs for the molecules CH_4, CH_3Cl, CH_3Br, and CH_3I, we observed similar peaks below the E_{Ps}.[38] The important clue that came out of that study was that these peaks were only observed in the three polar molecules, but not in the nonpolar CH_4 molecules. Following this previous observation, we also infer here that this structure at 1 eV for polar 1,1-$C_2H_2F_2$ is related to the dipole moment in these molecules and thus suggestive of a positron binding state. The scattering potential curves for positron scattering are still required which, if they should prove it true, would surely contribute towards solving the long standing proposition of the impossibility of resonances in positron scattering. (iii) Between the positronium formation (E_{Ps}) and ionization thresholds (E_{ion}), some weak structures are observed which should be due to electronic excitation. (iv) The opening up of the ionization channel at E_{ion} (10.49 eV) is followed by the rising up of the TCSs to produce the broad peak spanning the energy region up to about 60 eV. (v) Beyond 60 eV the TCSs decrease rather rapidly until, within experimental errors, they nearly equal the electron TCSs above 200 eV, i.e., a phenomenon expected since at these higher energies only the long-range interaction dominates the scattering event with the result that only the first Born term is sufficient for describing the scattering, where the square of the charge of the incoming particle comes into the cross-section formula leading to this convergence phenomenon in electron and positron TCSs. (vi) Except for the 1 eV peak feature, the absence of resonances in the positron TCSs is clearly observed in the low to intermediate energy ranges where the TCSs for electron impact are always larger by nearly a factor of about 1.5 in the region below 50 eV.

V. CONCLUSIONS

In this paper we present electron impact experimental TCSs and vibrational excitation DCSs, theoretical ECSs, and experimental positron impact TCSs for 1,1-$C_2H_2F_2$ molecules. Electron impact TCSs and ECSs show a rising trend below 0.8 eV attributed to the long-range dipole interaction. The minimum at about 1 eV in electron TCSs has been shown not to be a Ramsauer-Townsend minimum. Resonance peaks are observed at about 2.3, 6.5, 16, and 40 eV in both the electron TCSs and vibrational excitation DCSs. The Schwinger multichannel ECS results at the static-exchange and the static-exchange plus polarization approximations agree reasonably well above 20 eV. Agreement is observed between these experimental resonance peak positions with the theoretical results for the first three, and these have been assigned to the B_2, B_1, and A_1 symmetries, respectively. The 2.3 eV resonance is attributed to the shape resonance typical of a single C=C bond containing hydrocarbons. A comparative study of this resonance with those in C_2H_4 and C_2F_4 shows that the peak energy position shifts from 1.8 eV in C_2H_4, to 2.3 eV in 1,1-$C_2H_2F_2$, and 2.8 eV in C_2F_4; an observation attributed to the decreasing bond length. Positron TCSs show a decreasing trend below 1 eV, thus not revealing the expected long-range interaction effect for these polar 1,1-$C_2H_2F_2$ molecules. The larger magnitudes for electron TCSs than positron TCSs in the region below 50 eV are due to the resonances in the former not found in the latter, while the merging of these two sets of TCSs beyond 200 eV is expected from the first Born approximation.

ACKNOWLEDGMENTS

The work was supported in part by a Grant-in-Aid, the Ministry of Education, Science, Technology, Sport and Culture, Japan, the Japan Society for the Promotion of Science (JSPS), and the Japan Atomic Energy Research Institute (JAERI). One of the authors (C.M.) is also grateful to the JSPS for financial support under Grant No. P04064. Another author (H.T.) acknowledges Dr. T. Ozeki of the JAERI for his encouragement and support during this work. This work was also done under the International Atomic Energy Agency (IAEA) project for three of the authors (C.M., M.H., and H.T.). Two of the authors (M.H.F.B. and M.A.P.L.) acknowledge support from the Brazilian agency Conselho Nacional de Desenvolvimento Científico e Tecnológico (CNPq). MHFB also acknowledges support from the Paraná state agency Fundação Araucária and from FINEP (under Project No. CT-Infra 1). One of the authors (M.H.F.B.) also acknowledges Professor Carlos M. de Carvalho for computational support at Departamento de Física-UFPR. These calculations were made at CENAPAD-SP and a DF-UFPR.

[1] Kyoto Protocol to the United Nations Framework Convention on Climate Change, December 1997. See online publication at http://www.cnn.com/SPECIALS/1997/global.warming/stories/treaty.

This article is copyrighted as indicated in the article. Reuse of AIP content is subject to the terms at: http://scitation.aip.org/termsconditions. Downloaded to IP: 143.106.108.187 On: Thu, 18 Jun 2015 19:20:36

[2] Y. Mitsui, Y. Ohira, T. Yonemura, T. Takaichi, A. Sekiya, and T. Beppu, J. Electrochem. Soc. **151**, G297 (2004).
[3] R. Panajotovic, M. Kitajima, H. Tanaka, M. Jelisavic, J. Lower, L. Campbell, M. J. Brunger, and S. J. Buckman, J. Phys. B **36**, 1615 (2003).
[4] C. Szmytkowski, S. Kwitnewski, and E. Ptasinska-Denga, Phys. Rev. A **68**, 032715 (2003).
[5] L. M. Brescansin, L. E. Machado, and M.-T. Lee, Phys. Rev. A **57**, 3504 (1998).
[6] C. Winstead and V. McKoy, J. Chem. Phys. **116**, 1380 (2002); C. Winstead, V. McKoy, and M. H. F. Bettega, Phys. Rev. A **72**, 042721 (2005).
[7] M. J. Coggiola, W. M. Flicker, O. A. Mosher, and A. Kuppermann, J. Chem. Phys. **65**, 2655 (1976), and references therein.
[8] W. F. Edgell and W. E. Byrd, J. Chem. Phys. **17**, 740 (1949).
[9] D. C. Smith, J. R. Nielsen, and H. H. Classen, J. Chem. Phys. **16**, 326 (1950).
[10] P. Joyner and G. Glockler, J. Chem. Phys. **20**, 302 (1952).
[11] A. Roberts and W. F. Edgell, J. Chem. Phys. **17**, 742 (1949); Phys. Rev. **76**, 178 (1949).
[12] M. Allan, N. C. Craig, and L. V. McCarty, J. Phys. B **35**, 523 (2002).
[13] R. L. Wahl, *Principles and Practice of Positron Emission Tomography* (Lippincott, New York/Williams and Wilkins, Baltimore, 2002).
[14] P. J. Schultz and K. G. Lynn, Rev. Mod. Phys. **60**, 701 (1988).
[15] J. Mitroy, M. W. J. Bromley, and G. G. Ryzhikh, J. Phys. B **35**, R81 (2002).
[16] O. Sueoka, S. Mori, and A. Hamada, J. Phys. B **27**, 1452 (1994).
[17] M. Kimura, C. Makochekanwa, and O. Sueoka, J. Phys. B **37**, 1461 (2004).
[18] K. R. Hoffman, M. S. Dababneh, Y. F. Hsieh, W. E. Kauppila, V. Pol, J. H. Smart, and T. S. Stein, Phys. Rev. A **25**, 1393 (1982).
[19] O. Sueoka and S. Mori, J. Phys. B **19**, 4035 (1986).
[20] O. Sueoka, C. Makochekanwa, and H. Kawate, Nucl. Instrum. Methods Phys. Res. B **192**, 206 (2002).
[21] H. Tanaka, T. Ishikawa, T. Masai, T. Sagara, L. Boesten, M. Takekawa, Y. Itikawa, and M. Kimura, Phys. Rev. A **57**, 1798 (1998).
[22] S. K. Srivastava, A. Chutjian, and S. Trajmar, J. Chem. Phys. **63**, 2659 (1975).
[23] K. Takatsuka and V. McKoy, Phys. Rev. A **24**, 2473 (1981); **30**, 1734 (1984).
[24] M. H. F. Bettega, L. G. Ferreira, and M. A. P. Lima, Phys. Rev. A **47**, 1111 (1993).
[25] M. H. F. Bettega, A. P. P. Natalense, M. A. P. Lima, and L. G. Ferreira, J. Phys. B **36**, 1263 (2003).
[26] A. R. Lopes and M. H. F. Bettega, Phys. Rev. A **67**, 032711 (2003).
[27] M. T. do N. Varella, M. H. F. Bettega, M. A. P. Lima, and L. G. Ferreira, J. Chem. Phys. **111**, 6396 (1999).
[28] T. N. Rescigno, C. W. McCurdy, and B. I. Schneider, Appl. Phys. Lett. **63**, 248 (1989).
[29] C. Winstead and V. McKoy, Phys. Rev. A **57**, 3589 (1998).
[30] C. W. Bauschlicher, J. Chem. Phys. **72**, 880 (1980).
[31] *CRC Handbook of Chemistry and Physics*, 79th ed., edited by D. R. Lide (CRC, Boca Raton, FL, 1998).
[32] O. Sueoka and S. Mori, J. Phys. B **22**, 963 (1989).
[33] R. Panajotovic, M. Jelisavcic, R. Kajita, T. Tanaka, M. Kitajima, H. Cho, H. Tanaka, and S. J. Buckman, J. Chem. Phys. **121**, 4559 (2004).
[34] C. Winstead, Q. Sun, and V. McKoy, J. Chem. Phys. **96**, 4246 (1992).
[35] H. Kato, C. Makochekanwa, M. Hoshino, M. Kimura, H. Cho, T. Kume, A. Yamamoto, and H. Tanaka, Chem. Phys. Lett. **425**, 1 (2006).
[36] J. L. Carlos, Jr., R. R. Karl, Jr., and S. H. Bauer, J. Chem. Soc., Faraday Trans. 2 **2**, 177 (1974).
[37] N. S. Chiu, P. D. Burrow, and K. D. Jordan, Chem. Phys. Lett. **68**, 121 (1979).
[38] M. Kimura, O. Sueoka, C. Makochekanwa, H. Kawate, and M. Kawada, J. Chem. Phys. **115**, 7442 (2001).

This article is copyrighted as indicated in the article. Reuse of AIP content is subject to the terms at: http://scitation.aip.org/termsconditions. Downloaded to IP: 143.106.108.187 On: Thu, 18 Jun 2015 19:20:36